trilled crystals in other work is a strong indication that those particular samples were synthesized at a temperature near or above that for the onset of distortion from the hexagonal model with equally spaced metal atoms.

We further note that the results of refinement of $ZrCl_3$ in $P6_3/mcm$[10] suggest appreciably less distortion is present in that phase at room temperature than in the iodide. The smaller halide means zirconium–zirconium bonding is already significantly greater in the idealized $ZrCl_3$, 3.067 Å to two neighbors (total Zr–Zr bond order $n = 0.565$) relative to a 3.34-Å separation in the hypothetical ZrI_3 analogue ($n = 0.20$) and 3.172 Å to only one neighbor in the real iodide ($n = 0.38$ if the long separation is taken as nonbonding). The relative X-ray scattering by zirconium is significantly more important in the chloride than in the iodide, and yet the forced high-symmetry refinement of $ZrCl_3$ still gave fairly good R/R_w values, 3.0/4.4%, from a relatively large set of reflection data.[10] Recall that two studies of the iodide gave much more disparate residuals, 6.0/10.4%[10] and 3.7/11.9% (Table IV), appropriate to the dominance of iodine scattering. The temperature dependencies of the distortions in all of these structures should be interesting.

Other properties of most of these trihalides have not been well investigated. However, preliminary conductance and magnetic susceptibility data for the three ZrX_3 phases are certainly consistent with a metal-paired structure. Single-crystal conductivities at room temperature range between 2×10^{-5} ($ZrCl_3$) and 2×10^{-4} (ZrI_3) Ω^{-1} cm^{-1}, which are fairly comparable to values of 1×10^{-7} and 2.5×10^{-3} Ω^{-1} cm^{-1} for the corresponding NbX_4 phases where similar paired chains form via metal–metal bonding through shared edges of distorted halide octahedra. A strong localization of bonding electrons is implied for all. Magnetic data for the three zirconium halides[13,33] appear qualitatively consistent with the structural model after the effects of appreciable field-dependent impurities are removed; these all show a small paramagnetism that with decreasing temperature first increases slightly to moderately and then falls off markedly. The susceptibility of HfI_3 is also low and nearly temperature-independent down to 80 K.[16] The likely temperature dependencies of the metal–metal distances and thence of the energy gaps that pertain to both the conduction and the magnetic properties will obviously complicate analyses of the data.

Acknowledgment. Professor B. Krebs is thanked for discussions and the communication of unpublished structural results on several trihalides of this type during our investigations. Professor H. F. Franzen also provided helpful information and advice. This research was supported by the National Science Foundation, Solid State Chemistry, via Grants DMR-8318616 and -8902954 and was carried out in facilities of the Ames Laboratory, DOE.

Registry No. ZrI_3, 13779-87-8.

Supplementary Material Available: Tables of data collection and refinement information, distances, angles, and anisotropic thermal parameters for orthorhombic ZrI_3 (3 pages); a listing of F_o and F_c for the same structure (6 pages). Ordering information is given on any current masthead page.

(33) Baker, W. A.; Janus, A. R. *J. Inorg. Nucl. Chem.* **1964**, *26*, 2087.

Contribution from the Department of Chemistry,
Iowa State University, Ames, Iowa 50011

Encapsulation of the Platinum and Neighboring Metals within Cluster Iodides of Rare-Earth Elements

Martin W. Payne and John D. Corbett*

Received September 21, 1989

Syntheses of new cluster phases containing encapsulated heterometals have been explored through reactions between the rare-earth metal Y, Pr, or Gd (R), RI_3, and a 3d, 4d, or 5d element (Z) at 750–1000 °C in sealed Nb containers. New $Pr_7I_{12}Z$ ($Sc_7Cl_{12}N$-type) phases are obtained for Z = Cu, Ru, Rh, Pd, Re, Os, Ir, and Pt. New $Gd_7I_{12}Z$ phases occur for Z = Ni, Cu, Ru, Rh, Pd, Os, Ir, Pt, and Au. In contrast, new $Y_6I_{10}Z$ analogues of the previously reported $Y_6I_{10}Ru$ occur with Z = Co, Ni, Rh, Os, Ir, and Pt and as $Pr_6I_{10}Os$. The structures of $Y_6I_{10}Os$ and $Y_6I_{10}Ir$ have been refined for comparison with $Y_6I_{10}Ru$ ($P\bar{1}$, $Z = 1$; $a = 7.6268$ (8), 7.6154 (7) Å, $b = 9.518$ (1), 9.535 (1) Å, $c = 9.617$ (1), 9.577 (1) Å, $\alpha = 107.72$ (1), 107.67 (1)°, $\beta = 97.17$ (1), 97.11 (1)°, $\gamma = 105.13$ (1), 105.15 (1)°; $R/R_w = 3.1/4.2$, 3.7/4.3%, respectively). The sizable tetragonal compression observed earlier in the $Y_6I_{10}Ru$ cluster and thought to be electronically driven is only 44% as great in the isoelectronic Os phase and is virtually absent in $Y_6I_{10}Ir$. Relativistic effects may be important in the bonding of the 5d interstitials. Unsuccessful syntheses, orbital populations in the various clusters, volume changes seen among the $R_7I_{12}Z$ phases, and matrix effects in intercluster bonding are also discussed and interrelated.

Introduction

Exploratory synthesis can in the best of times provide a continuing series of surprises. For instance, once the concept was clear that interstitial atoms (Z) afforded new cluster[1] and condensed cluster[2,3] halides of the early transition metals, a large and diverse family of zirconium cluster chloride stoichiometries and structures were synthesized. These were all based on $Zr_6Cl_{12}Z$ units in which one of a relatively small group of atoms was bonded, H or Be–N.[4,5] Use of the iodides instead gave $Zr_6I_{12}Z$-type cluster phases that also encapsulated heavier main-group elements, Al, Si, Ge, or P.[6,7] Shortly later, 3d metals were found to bind within zirconium clusters, first for Cr–Co in iodides[8] and later for Mn–Ni in the chlorides.[9] Most of these examples can be interpreted fairly well with the aid of simple extended Hückel calculations and in

(1) Smith, J. D.; Corbett, J. D. *J. Am. Chem. Soc.* **1985**, *107*, 5704.
(2) Ford, J. E.; Corbett, J. D.; Hwu, S.-J. *Inorg. Chem.* **1983**, *22*, 2789.
(3) Hwu, S.-J.; Corbett, J. D.; Poeppelmeier, K. R. *J. Solid State Chem.* **1985**, *57*, 43.
(4) Ziebarth, R. P.; Corbett, J. D. *J. Am. Chem. Soc.* **1989**, *111*, 3272 and references therein.
(5) Ziebarth, R. P.; Corbett, J. D. *Acc. Chem. Res.* **1989**, *22*, 256.
(6) Smith, J. D.; Corbett, J. D. *J. Am. Chem. Soc.* **1986**, *108*, 1927.
(7) Rosenthal, G.; Corbett, J. D. *Inorg. Chem.* **1988**, *27*, 53.
(8) Hughbanks, T.; Rosenthal, G.; Corbett, J. D. *J. Am. Chem. Soc.* **1988**, *110*, 1511.
(9) (a) Rogel, F.; Zhang, J.; Payne, M. w.; Corbett, J. D. *Adv. Chem. Ser.* **1990**, *No. 226*, 369. (b) Zhang, J.; Corbett, J. D. Unpublished research.

0020-1669/90/1329-2246$02.50/0

terms of strong bonding between the host (cluster) metal and the interstitial atom.

The next breakthrough occurred when centered 3d elements Mn–Ni were found to stabilize new $R(R_6I_{12}Z)$ phases of several rare-earth metals (R),[10] cluster types for which relatively few examples have been found with encased light elements other than carbon.[11,12] At the same time, a series of condensed cluster phases of the same elements were uncovered that contain B, C, or N.[3,13] The discovery of metal clusters that bind centered heterometal atoms gave the first glimpses of a family of fairly simple compounds in which small fragments of intermetallic compounds and their bonding could be regularly isolated, in these cases sheathed by a protective layer of halide. Interestingly, the cluster metal–Z separations in many centered clusters were found to be noticeably smaller than in their intermetallic counterparts.

The next revelation involved the capture of a heavier transition metal in the phases $Y_7I_{12}Ru$ and $Y_6I_{10}Ru$.[14] The latter revealed a new and especially interesting structure in which isolated $Y_6(Ru)I_{12}$ clusters share four inner iodine atoms to form chains. A marked tetragonal compression of the cluster was thought to be associated with electronic effects for this particular cluster electron count.

We have since expanded our search for other heavy transition-metal atoms encapsulated within rare-earth-metal iodide clusters and have found that Nature is again generous. For the R elements sampled, Y, Pr, and Gd, we here report that the interstitials Cu, Ru–Pd and Re–Au can also be bound in a $R_6I_{12}Z$ cluster in either an $R_7I_{12}Z$ or an $R_6I_{10}Z$ phase. Thus, possible transition-metal interstitials Z in these compounds now include all of the elements

Mn	Fe	Co	Ni	Cu
	Ru	Rh	Pd	
Re	Os	Ir	Pt	Au

Although most occur for more than one R example, significant differences in stability are still found among the limited range of host elements studied. The crystal structures of two compounds, $Y_6I_{10}Os$ and $Y_6I_{10}Ir$, have also been refined for comparison with the distorted ruthenium analogue noted above.

Experimental Section

Materials. The high purity of the rare-earth metals used as well as the synthetic and vacuum sublimation techniques for the corresponding RI_3 phases and the 3d-metal iodides have been described before.[10,13] Most of the yttrium employed was a vacuum-sublimed Johnson-Matthey/AESAR product (99.99%, metal basis), and the powdered metal was prepared via the hydride.[13] Finely powdered Pt, Ag (Fisher), Cr, V, Re, Os, Pd, Ir (AESAR), Ru, Au (Engelhard), and W (Alfa) were used. The iodides of V–Cu and Ag were also employed as potential interstitial sources. The phases Pr_3Ru and Gd_3Ru were prepared by arc melting and likewise tested for comparison.

Syntheses. The $R_7I_{12}Z$ phases as well as the $Y_6I_{10}Z$ and $Pr_6I_{10}Os$ products were obtained for R = Y, Pr, and Gd as before[3,10] via reactions of stoichiometric proportions of RI_3, R, and either powdered elemental Z or its iodide in welded Nb containers. Reaction temperatures in the range 750–1000 °C and periods of 1–5 weeks were explored. Most of the new compounds are obtained in ≥80% yield in the range 800–950 °C. Some obvious exceptions are $Pr_7I_{12}Re$ and $Pr_7I_{12}Pt$, for which 900 and 875 °C, respectively, appear too high, and $Pr_7I_{12}Cu$, for which 850 °C (70% yield) is better than 800 °C. The source of Z—powdered element, iodide, or R_3Z—does not seem to have a significant effect. Yields of stoichiometrically loaded reactions run at the higher temperatures are often decreased because of the formation of ROI through intrusion of oxygen from R,[15] the container, or the silica jacket.

Table I. Lattice Constants (Å) and Cell Volumes (Å^3) of New $R_7I_{12}Z$ Phases[a]

compd	no. of lines	*a*	*c*	*V*	previously reported Z[b]
$Pr_7I_{12}Cu$	42	15.853 (2)	10.668 (2)	2321.7 (7)	Mn, Fe, Co, Ni
$Pr_7I_{12}Ru$	54	15.883 (1)	10.769 (1)	2352.9 (4)	
$Pr_7I_{12}Rh$	54	15.910 (2)	10.733 (2)	2352.8 (7)	
$Pr_7I_{12}Pd$	38	15.851 (2)	10.705 (1)	2329.2 (6)	
$Pr_7I_{12}Re$	36	15.929 (3)	10.777 (2)	2368.2 (8)	
$Pr_7I_{12}Os$	60	15.910 (2)	10.806 (3)	2368.9 (8)	
$Pr_7I_{12}Ir$	64	15.930 (2)	10.724 (2)	2357.0 (6)	
$Pr_7I_{12}Pt$	37	15.931 (3)	10.776 (3)	2369 (1)	
$Gd_7I_{12}Ni$	36	15.518 (2)	10.534 (2)	2196.7 (6)	Mn, Fe, Co
$Gd_7I_{12}Cu$	50	15.5188 (8)	10.4435 (9)	2178.2 (3)	
$Gd_7I_{12}Ru$	38	15.572 (1)	10.553 (1)	2216.2 (4)	
$Gd_7I_{12}Rh$	35	15.581 (1)	10.535 (1)	2214.9 (4)	
$Gd_7I_{12}Pd$	68	15.5817 (9)	10.550 (1)	2218.3 (4)	
$Gd_7I_{12}Os$	31	15.586 (1)	10.570 (2)	2223.6 (6)	
$Gd_7I_{12}Ir$	29	15.5802 (9)	10.557 (1)	2219.4 (4)	
$Gd_7I_{12}Pt$	50	15.6041 (6)	10.5488 (9)	2224.4 (3)	
$Gd_7I_{12}Au$	34	15.640 (1)	10.484 (1)	2220.9 (4)	

[a] Space group $R\bar{3}$ (hexagonal setting, $Z = 3$), $Sc_7Cl_{12}N$-type. Based on Guinier powder data with Si as an internal standard; $\lambda = 1.54056$ Å. [b] Reference 10.

Among the systems studied, the $R_6I_{10}Z$ phases seem to be significant alternatives to $R_7I_{12}Z$ only for yttrium and with $Pr_6I_{10}Os$. Similar to earlier observations on $Y_7I_{12}Ru$ vs $Y_6I_{10}Ru$,[13] the $R_6I_{10}Z$ version is favored by longer reaction periods or higher temperatures when both phases occur in the same system. The product distribution in these cases is also somewhat responsive to the stoichiometry loaded.

Negative experiments are also important in synthetic explorations, and the following interstitial candidates have so far not yielded new phases in either of these structures. Y: V, Cr, Mn, Zn, Cu, Mo, Pd, Ag, Cd, Re, Au. Pr: V, Cr, Cu, Zn, Mo, Ag, Au. Gd: V, Cr, Zn, Mo, Ag, Cd, Re. Low-yield syntheses of $R_7I_{12}Z$ phases with unusually small lattice constants were occasionally encountered. These circumstances again[7] point to adventitious impurities functioning as Z, carbon especially. It should be noted that just 56 μg of carbon is required to give a 5% yield of $Y_7I_{12}C$ from a reaction run on a 200-mg scale. The well-crystallized product at this level is easy to locate and separate under a low-power microscope.

Powder X-ray Studies. The above phases (as well as other products) were readily identified by comparison of the powder patterns calculated[16] with the aid of the atom parameters in $Y_7I_{12}Fe$ or $Y_6I_{10}Ru$ (or other) with those measured with the aid of an Enraf-Nonius (FR-552) Guinier camera. Protection of the samples between layers of Scotch tape has been described earlier.[17] Powdered silicon (NBS/NIST) was included with each sample in order to provide an internal calibration of the film. Lattice constants of each new phase were then obtained by standard least-squares refinement of measured and indexed reflections in its pattern. The lattice parameter results for all of the new $R_7I_{12}Z$ and $R_6I_{10}Z$ phases synthesized in the course of this research are listed in Tables I and II along with the number of lines refined and the unit cell volume of each.

Single-Crystal X-ray Studies. The structures of $Y_6I_{10}Os$ and $Y_6I_{10}Ir$ were defined to allow comparison with that of the unusual $Y_6I_{10}Ru$. Diffraction data from 0.20 × 0.20 × 0.40 and 0.26 × 0.20 × 0.22 mm crystals sealed in thin-walled capillaries were measured at 23 °C and to $2\theta = 55°$ and 70°, respectively, on a Rigaku AFC6R diffractometer. Empirical absorption corrections (DIFABS[18]) were applied to both data sets, since the absorption coefficients are quite large. Refinements starting with parameters for the ruthenium parent proceeded normally. Secondary extinction corrections were important. Programs utilized were those in the instrument package TEXSAN, which also includes the scattering factors with real and imaginary corrections for anomalous dispersion. Some pertinent data are listed in Table III. The heavy atoms refined to occupancies of 99.4 (2) (Os) and 100.9 (3)% (Ir). The final difference maps were flat to 1.7 and 3.4 e/Å^3, respectively, both residuals being close to the heaviest atoms. The data set for the osmium compound appeared to exhibit the effects of series termination; some reflections were still strong at the $2\theta = 55°$ limit. The ellipsoid components for Ir were particularly small along $\vec{b}$ and $\vec{c}$ (5:1:1), an effect that does not seem to

(10) Hughbanks, T.; Corbett, J. D. *Inorg. Chem.* **1988**, *27*, 2022.
(11) Simon, A. *J. Solid State Chem.* **1985**, *57*, 2.
(12) Hwu, S.-J.; Corbett, J. D. *J. Solid State Chem.* **1986**, *64*, 331.
(13) Kauzlarich, S. M.; Hughbanks, T.; Corbett, J. D.; Klavins, P.; Shelton, R. N. *Inorg. Chem.* **1988**, *27*, 1791.
(14) Hughbanks, T.; Corbett, J. D. *Inorg. Chem.* **1989**, *28*, 631.
(15) Corbett, J. D.; Smith, J. D.; Garcia, E. *J. Less-Common Met.* **1986**, *115*, 343.
(16) Clark, C. M.; Smith, D. K.; Johnson, G. J. *A Fortran II Program for Calculating X-Ray Diffraction Patterns-Version 5*; Department of Geosciences, Pennsylvania State University: University Park, PA, 1973.
(17) Daake, R. L.; Corbett, J. D. *Inorg. Chem.* 1978, *17*, 1192.
(18) Walker, N.; Stuart, D. *Acta Crystallogr., Sect. A* **1983**, *A39*, 159.

Table II. Lattice Constants (Å and deg) and Cell Volumes (Å^3) of $R_6I_{10}Z$ Phases[a]

compd	no. of lines	a	b	c	α	β	γ	V
$Y_6I_{10}Co$	99	7.5877 (9))	9.483 (1)	9.5174 (8)	107.563 (8)	97.106 (9)	105.11 (1)	614.9 (1)
$Y_6I_{10}Ni$	91	7.5817 (8)	9.500 (1)	9.5113 (9)	107.54 (1)	97.08 (1)	105.10 (1)	615.3 (1)
$Y_6I_{10}Ru$[b]	51	7.627 (1)	9.461 (2)	9.640 (2)	107.82 (2)	97.21 (2)	105.02 (2)	623.6 (2)
$Y_6I_{10}Rh$	53	7.6141 (9)	9.518 (1)	9.568 (1)	107.62 (1)	97.11 (1)	105.14 (1)	622.2 (1)
$Y_6I_{10}Os$	83	7.6268 (8)	9.518 (1)	9.617 (1)	107.72 (1)	97.17 (1)	105.13 (1)	625.9 (1)
$Y_6I_{10}Ir$	112	7.6154 (7)	9.535 (1)	9.577 (1)	107.67 (1)	97.11 (1)	105.15 (1)	623.8 (1)
$Y_6I_{10}Pt$	99	7.6128 (5)	9.5632 (7)	9.5804 (6)	107.640 (6)	97.072 (7)	105.181 (7)	625.76 (7)
$Pr_6I_{10}Os$	58	7.8893 (9)	9.786 (2)	9.871 (2)	108.23 (2)	97.40 (1)	105.74 (1)	677.3 (2)

[a] Space group $P\bar{1}$, $Z = 1$, $Y_6I_{10}Ru$ type; $\lambda = 1.540\,56$ Å. [b] Previously reported[14] from fewer lines.

Table III. Data Collection and Refinement Parameters for $Y_6I_{10}Z$[a]

compd	$Y_6I_{10}Os$	$Y_6I_{10}Ir$
space group, Z	$P\bar{1}$, 1	$P\bar{1}$, 1
T, °C	23	23
μ, cm^{-1} (Mo Kα)	322.6	323.6
transm coeff range	0.88–1.17	0.87–1.19
R[b]	3.1	3.7
R_w[b]	4.2	4.3

[a] $Y_6I_{10}Ru$ structure type.[14] Unit cell parameters are given in Table II. [b] $R = \sum||F_o| - |F_c||/\sum|F_o|$; $R_w = [\sum w(|F_o| - |F_c|)^2/\sum w(F_o)^2]^{1/2}$; $w = 1/\sigma(F_o^2)$.

Table IV. Positional Parameters for $Y_6I_{10}Z$ Phases[a]

atom	x	y	z	B_{eq}, Å^2
		$Y_6I_{10}Os$		
Y1	0.040 01 (9)	−0.246 64 (8)	0.114 8 (1)	0.54 (2)
Y2	0.284 3 (1)	0.085 20 (8)	−0.027 2 (1)	0.68 (2)
Y3	0.131 37 (9)	0.171 04 (8)	0.359 1 (1)	0.55 (2)
I1	0.462 44 (7)	0.277 82 (7)	0.361 48 (8)	1.44 (2)
I2	0.091 25 (7)	0.467 35 (6)	0.268 97 (8)	1.35 (2)
I3	0.372 66 (6)	−0.182 55 (6)	0.088 36 (9)	1.32 (2)
I4	−0.187 83 (6)	0.093 11 (6)	0.450 27 (7)	0.76 (2)
I5	0.268 23 (6)	0.356 49 (6)	−0.208 26 (8)	0.83 (2)
Os	0	0	0	0.21 (1)
		$Y_6I_{10}Ir$		
Y1	0.039 8 (1)	−0.244 51 (8)	0.114 7 (1)	0.42 (2)
Y2	0.288 1 (1)	0.087 36 (8)	−0.027 6 (1)	0.52 (2)
Y3	0.129 5 (1)	0.169 58 (8)	0.355 7 (1)	0.44 (2)
I1	0.462 51 (7)	0.277 81 (7)	0.362 87 (8)	1.39 (2)
I2	0.090 95 (8)	0.468 05 (6)	0.268 03 (7)	1.32 (2)
I3	0.373 47 (7)	−0.183 58 (6)	0.087 94 (9)	1.29 (2)
I4	−0.187 72 (7)	0.093 87 (6)	0.451 48 (7)	0.73 (1)
I5	0.266 96 (7)	0.356 65 (5)	−0.212 35 (7)	0.79 (2)
Ir	0	0	0	0.151 (6)

[a] Space group $P\bar{1}$.

depend on the absorption correction method.

Positional and the isotropic equivalent ellipsoid data for $Y_6I_{10}Os$ and $Y_6I_{10}Ir$ are given in Table IV; other information on the data collections and refinements, the anisotropic displacement parameters, and the structure factor results are available as supplementary material.

Results and Discussion

The extensive results provided by this investigation are best presented and discussed in five categories: (1) the synthetic results and the implicit stability ranges of the $R_7I_{12}Z$ and $R_6I_{10}Z$ compounds; (2) unsuccessful reactions and what these imply about cluster stability and alternate phases; (3) the range of cluster-based electron counts found among cluster iodides that contain transition metals; (4) the refined structural results for $Y_6I_{10}Os$ and $Y_6I_{10}Ir$ and their comparison with that of the parent $Y_6I_{10}Ru$, especially regarding cluster distortions; (5) trends in the cell volumes for the 27 $R_7I_{12}Z$ phases and their implications regarding cluster and interstitial sizes.

Syntheses. The surprising versatility of the rare-earth-metal clusters in bonding transition metals as interstitials is emphasized by the present results. Among the three host elements we sampled—Y, Pr, and Gd—the two lanthanides show the greater range of interstitials Z in the $R_7I_{12}Z$ composition, as follows:

		16	17	18	19	20
$Pr_7I_{12}Z$:	Z =	Mn	Fe	Co	Ni	Cu
			Ru	**Rh**	**Pd**	
		Re	**Os**	**Ir**	**Pt**	

and

		16	17	18	19	20
$Gd_7I_{12}Z$:	Z =	Mn	Fe	Co	**Ni**	Cu
			Ru	**Rh**	**Pd**	
			Os	**Ir**	**Pt**	**Au**

The new results are shown in bold face type, while the others were reported earlier.[10] The number of cluster-based electrons that are listed as a heading to each group will be considered later. Several attempts to incorporate each of the neighboring elements V, Cr, Mo, W, Ag, Zn, and Cd were unsuccessful.

The situation with yttrium is markedly different because a second cluster phase, $Y_6I_{10}Z$, has comparable stability. The distribution of yttrium clusters between the two structures is as follows, with Z examples for $Y_7I_{12}Z$ on the upper left, $Y_6I_{10}Z$ on the lower right, and both phases with Ru and Co (dashed line):

	17	18	19	
$Y_7I_{12}Z$:	Fe	Co	Ni	
	Ru	Rh		
	Os	**Ir**	**Pt**	: $Y_6I_{10}Z$
	16	17	18	

(The $Y_7I_{12}Co$ portion of the pair was reported before.[10]) The $Y_7I_{12}Z$ and $Y_6I_{10}Z$ stoichiometries and stabilities for Z = Ru and Co are sufficiently close that either, or sometimes both, can be found in reactions loaded for the stoichiometry of either. The $Y_6I_{10}Z$ member of each pair becomes predominant at higher temperatures or after longer reaction periods, suggesting that the stability of the alternative $Y_7I_{12}Z$ is more kinetic than thermodynamic in character. Negative results with yttrium in either structure have been obtained regularly with V, Cr, Mo, W, Mn, Re, Cu, Ag, Au, Zn, and Cd.

The substantial differences between the gadolinium and yttrium products found in this study are noteworthy considering the frequently assumed similarities of these two elements. Notable dimensional differences have been noted between the isostructural Gd_2Cl_3 and Y_2Cl_3,[19] 0.07–0.10 Å, in spite of the very similar metallic radii usually cited.[20] Significant electronic differences must be present as well to account for the striking differences in phase stability found here, especially in the greater variety of Z taken up in the gadolinium clusters.

The subtleties that govern the distribution of clusters between the $R_6I_{10}Z$ and the $R_7I_{12}Z$ structure types are beyond our ken at

(19) Mattausch, Hj; Hendricks, J. B.; Eger, R.; Corbett, J. D.; Simon, A. *Inorg. Chem.* **1980**, *19*, 2128.
(20) Pauling, L. *The Nature of the Chemical Bond*, 3rd ed.; Cornell University Press: Ithaca, NY, 1960; pp 403, 410.

the moment except perhaps for nickel and platinum. In these cases, the $Y_6I_{10}Z$ choice does achieve the apparently optimal 18-electron cluster count indicated by extended Hückel calculations (below).[8,10] (Palladium does not form the analogous compound, however.) The opportunity to form shorter and stronger intercluster bridging $Y-I^{a-i}$ bonds with the larger Ru in $Y_6I_{10}Ru$ once seemed important, but this appears less significant now that small interstitials have been incorporated in $Y_6I_{10}Co$ and $Y_6I_{10}Ni$.

The Z elements taken up in these syntheses are likely transported via the gaseous iodides, perhaps at relatively low pressures, since metallic R or a strongly reducing RI_2 is often present as well. The experimental conditions employed do appear to produce equilibrium systems in most cases. Use of the reactants ZI_x or R_nZ in place of Z probably serve mainly as a means of producing finely divided Z during the early stages of reaction.

Unsuccessful Attempts. An unsuccessful reaction is, generally speaking, easy to recognize, as it characteristically yields a simple binary RI_n phase as well as unreacted metal. (The product of Z is usually in too small an amount to be located.) However, each of the three R elements studied provides a different iodide in these cases. The only binary iodide known for yttrium is YI_3, while unsuccessful reactions with PrI_3 give a variety of reduced iodides: Pr_2I_5[21,22] as well as varying amounts of three forms of PrI_2, the $TiSi_2$ (or $MoSi_2$) type,[21] the rhombohedral 3R-MoS_2 type, and the Pr_4I_8 ($Mo_4S_4Br_4$) cluster structure (forms 1, 3, 5).[23] Similarly, reactions of GdI_3 that fail to produce octahedral clusters give the metallic GdI_2 but only in the 2H-MoS_2 structure.[21] All of these diiodides are probably stable with respect to disproportionation by only a few kilocalories per mole, so that they provide only small competition to the formation of the cluster iodides. On the other hand, the presence of a more stable, saltlike diiodide such as DyI_2, and presumably other factors as well, do preclude the formation of $Dy_7I_{12}Z$ compounds with Fe or Co interstitials.[10] The same is expected for other elements that form the more stable diiodides, namely for Sm, Eu, Tm, Yb, and possibly Nd. Naturally, even subtle differences that involve only small energy changes can make the difference between stability and instability of a solid phase.

The lack of success in inserting a given element into a cluster host cannot be simply interpreted to mean that some particular parameter of just the cluster is responsible, for example the strength of the R–Z bonding, an extreme H_{ii} value for Z, the size of Z, or their combination, although such simplifications are sometimes invoked. *The stability of a compound in a equilibrium system is always relative to the stability of alternative phases.* A particular diversity in the alternative can result with a series of interstitials from the same period, since in these cases the different Z may have very different chemistries. Thus, the course of reactions with Cr, Mn, Fe, etc. depend on the relative stabilities of not just these elements, or their iodides, but also the intermetallic compounds they each form with a given rare-earth-element host, and the last may vary markedly across the series. Comparisons and predictions about the behavior of different R elements with fixed Z, as above, or of fixed R with a family of Z elements are presumably governed by more regular trends.

Electron Count and Stability. The role of the interstitial is to provide both electrons and orbitals for the formation of strong bonds with the d orbitals of the skeletal metal. The bonding scheme has been considered several times via extended Hückel MO calculations. Experimentally, a closed-shell configuration ($14e^-$) is achieved in about 85% of the zirconium cluster chlorides centered by a main-group element, and a similar result ($18e^-$) pertains to those containing 3d elements.[4,9] Examples that contain one or two additional electrons are more readily achieved for the zirconium iodides encapsulating main-group interstitials. An interpretation of most of these exceptions as well as those seen with traditional niobium and tantalum halide clusters has recently been put forth in terms of matrix effects that diminish the antibonding character of the a_{2u} orbital, normally the LUMO, for large X, small Z, or small host metal.[4]

Cluster iodides centered by transition metals exhibit a somewhat different pattern and less regularity. The relevant MO's for a rare-earth-metal iodide with an iron interstitial scale approximately as follows:

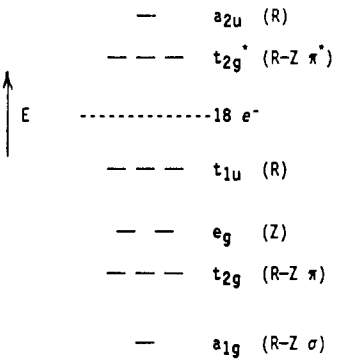

This diagram differs from that with a main-group interstitial by (a) the addition of the nonbonding e_g^4 set on the centered transition metal, (b) the bonding nature of t_{2g}^6 involving both the cluster and Z, and (c) the virtual nonbonding HOMO character of t_{1u}^6 orbital since the p orbitals on these Z generally lie too high in energy to be effective.[8,10,14] Nonetheless, the 18-electron "rule" suggested by this diagram is much less applicable to the present cluster iodides (the chloride analogues are not known). Cluster examples that span 16–20 electrons are known among the $R_7X_{12}Z$ phases, although the range is only 16–$18e^-$ in $Y_6I_{10}Z$ compounds (above). The MO scheme probably varies in detail for this relatively large range of Z examples, at least in part because of the varying sizes and valence-state orbital energies.

Two generalities regarding the stable electron configurations come to mind. First, these large interstitials may expand the clusters so much that the normal t_{1u}^6 HOMO, which is only R–R bonding,[10] is virtually nonbonding and allows the loss of one or two electrons. (The average Y–Y distance in $Y_6I_{10}Os$ corresponds to a bond order of only 0.11.) This may be enhanced by the high polarity of the R–Z interactions in these compounds, which places the t_{1u} level higher with respect to the R–Z bonding components a_{1g}^6 and t_{2g}^6 and the nonbonding e_g^4 on Z. Clearly, the lack of good structural alternatives with fewer iodides is necessary for the electron poorer 16- and $17e^-$ examples to form. Second, the valence-state energies of the later Z will be distinctly lower, with less mixing the R and more charge on Z. This means t_{2g}^* will also fall, perhaps because of poorer R–Z overlap as well. At the same time, t_{1u}^6 is only R–R bonding (in the absence of useful p orbitals on Z) and remains fairly constant. This decreasing gap presumably is involved in the stability of 19- and $20e^-$ clusters in the appropriate cases although, again, many other factors are involved as well. The lack of stable, alternate structures and compositions as are found with $Zr_6I_{14}Z$[1,6] is implicit in these arguments.

The effects of alternative trigonal distortions of clusters in $R_7I_{12}Z$ phases are unknown; however, structural data for $R_7X_{12}Z$ phases for Z = H, B, N, Fe, and Co suggest that these distortions may depend on packing a good deal more than on electron count.[10,12] Relatively extensive structural studies and calculations would be necessary to understand these subtle details and put these electronic rationalizations on a firmer basis.

$Y_6I_{10}Z$ Phases and Cluster Distortions. This phase is iodine-poor relative to those containing the usual M_6X_{12} building blocks, with four inner (edge-bridging) iodine atoms (I^i) shared between clusters to form chains of hypoclusters, viz., $Y_6(Z)I^i_8I^{i-i}_{4/2}$. The cluster interconnections in the other two directions involve pairs of the more common $R-I^{i-a}$--R interactions in which an inner halide in one cluster is bonded exo to an R vertex in another. This stoichiometry, first discovered for $Y_6I_{10}Ru$,[14] has now been extended to yttrium examples with six other Z elements, but only one member appears to be stable for the other two R hosts examined, namely $Pr_6I_{10}Os$.

(21) Warkentin, E.; Bärnighausen, H. Unpublished research.
(22) Schleid, T.; Meyer, G. *Z. Anorg. Allg. Chem.* **1987**, *552*, 97.
(23) Warkentin, E.; Bärnighausen, H. *Z. Anorg. Allg. Chem.* **1979**, *459*, 187.

Table V. Important Distances (Å) and Angles (deg) in $Y_6I_{10}Os$ and $Y_6I_{10}Ir$

distance	Os	Ir
Y1–Y2	3.797 (1)	3.809 (1)
Y1–Y2[a]	3.787 (1)	3.808 (1)
Y1–Y3	3.928 (1)	3.892 (1)
Y1–Y3[a]	3.803 (1)	3.777 (1)
Y2–Y3	3.916 (2)	3.727 (1)
Y2–Y3[a]	3.710 (1)	3.935 (1)
Y1–Z	2.7179 (8)	2.6947 (7)
Y2–Z	2.6438 (9)	2.6912 (9)
Y3–Z	2.750 (1)	2.7283 (8)
Y1–Y2	3.083 (1)	3.093 (1)
Y1–I2[b]	3.232 (1)	3.2395 (9)
Y1–I3	3.094 (1)	3.122 (1)
Y1–I4	3.190 (1)	3.184 (1)
Y1–I5	3.094 (1)	3.113 (1)
Y2–I1	3.022 (1)	3.027 (1)
Y2–I3	3.091 (1)	3.105 (1)
Y2–I3[b]	3.278 (1)	3.247 (1)
Y2–I4	3.201 (1)	3.215 (1)
Y2–I5	3.116 (1)	3.1205 (9)
Y3–I1	2.989 (1)	3.009 (1)
Y3–I2	3.114 (1)	3.1198 (9)
Y3–I4	3.184 (1)	3.188 (1)
Y3–I4	3.173 (1)	3.1894 (9)
Y3–I5[b]	3.252 (1)	3.2577 (9)
I2[b]–I4[c]	4.188 (1)	4.174 (1)
I2[b]–I5	4.195 (1)	4.188 (1)
I3[b]–I3	4.198 (1)	
I3[b]–I4	4.177 (1)	4.196 (1)
I3[b]–I5	4.178 (1)	4.188 (1)
I1–I2[d]	4.194 (1)	
I1–I4[d]	4.163 (1)	4.167 (1)
I1–I5[d]	4.160 (1)	4.157 (1)
I2–I2		4.197 (1)
angle	**Os**	**Ir**
Y1–Z–Y3	91.85 (3)	91.71 (2)
Y1–Z–Y2	90.15 (3)	90.01 (2)
Y2–Z–Y3	86.91 (3)	86.88 (3)
I2–Y1–I4	164.99 (3)	164.01 (3)
I3–Y1–I5	166.09 (3)	164.93 (3)
I1–Y2–I4	164.48 (3)	165.79 (3)
I3–Y2–I5	162.54 (3)	163.23 (3)
I1–Y3–I4	167.49 (3)	166.21 (3)
I2–Y3–I4	166.56 (3)	165.87 (2)
Z–Y1–I2	177.63 (5)	177.91 (9)
Z–Y2–I3	176.51 (6)	176.50 (5)
Z–Y3–I5	176.01 (6)	176.31 (3)
Y1–I4–Y3	76.09 (3)	75.27 (2)
Y1–I4–Y3	96.57 (3)	97.03 (3)
Y2–I4–Y3	75.81 (3)	75.84 (3)
Y2–I4–Y3	96.53 (3)	96.67 (2)
Y3–I4–Y3	92.60 (3)	92.50 (2)

[a] Inversion-related atom. [b] Exo I^{a-i}. [c] Only $d(I–I) \leq 4.20$ Å are listed. [d] Intercluster $d(I^i–I^i)$.

An unusual distortion was found in $Y_6I_{10}Ru$, substantially a tetragonal compression that makes the two Y2–Ru distances a full 0.20 Å less than the other four. The distortion appears to have little to do with the chain condensation that occurs along one of the basal plane directions. Extended Hückel calculations suggested a rationalization of this in terms of favorable bonding interactions between yttrium 4d orbitals that split the t_{1u}^4 HOMO into a two-below-one pattern. The more common Y–Ru contributions to bonding in this representation were found to be truly negligible because the 5p valence orbitals on the interstitial lie so high in energy.[14]

A question naturally arose as to whether the distortion observed in $Y_6I_{10}Ru$ is general and correctly interpreted, since the structure has been found for clusters over a 16–18-electron range. We therefore refined the structures of the isoelectronic $Y_6I_{10}Os$ and

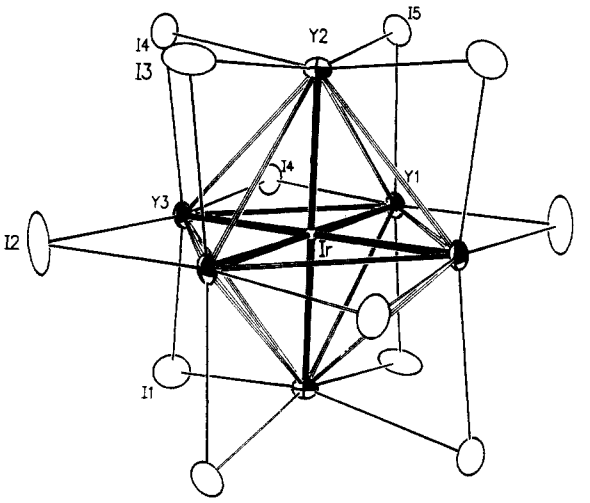

Figure 1. Centric $Y_6(Ir)I_{12}$ cluster unit in $Y_6I_{10}Ir$, with Y–Ir bonding emphasized (90% probability thermal ellipsoids, Ir isotropic). Yttrium and iodine atoms are the shaded and open ellipsoids, respectively. The I4 atoms have an edge-bridging function in adjoining clusters as well.

Table VI. Pertinent Bond Distances (Å) According to Bond Type in $Y_6I_{10}Z$, Z = Ru, Os, and Ir[a]

	Ru[b]	Os	Ir
	Yttrium–Interstitial		
Y1–Z	2.752	2.718	2.695
Y2–Z	2.556	2.644	2.691
Y3–Z	2.772	2.750	2.728
Δd (odd axis member)	–0.206 (Y2)	–0.090 (Y2)	+0.035 (Y3)
$\bar{d}$	2.693	2.704	2.705
	Yttrium–Iodine		
$\bar{d}(Y–I^a)$	3.262	3.254	3.248
Δd (odd axis member)	+0.065 (Y2)	+0.036 (Y2)	+0.014 (Y3)
$\bar{d}(Y–I^i)$	3.117	3.113	3.124
electron count	16	16	17

[a] $\sigma_d \times 10^3$ values are ≤ 4, 1, and 1 for the Ru, Os, and Ir structures, respectively. [b] Ru data from ref 14.

of the 17-electron $Y_6I_{10}Ir$ for comparison, only to discover that the characters of the distortions in these are rather different. The positional parameters as well as the isotropic equivalent ellipsoids for the atoms in these appear in Table IV,[24] while important distances and angles therein are given in Table V. The centric cluster in $Y_6I_{10}Ir$ is depicted in Figure 1.

Marked changes in Y–Z interactions are the only features that distinguish among the three structures. Some relevant data are compared in Table VI. The averages for Y–Z and for the radially opposed $Y–I^a$ change scarcely at all. The striking 0.20 Å shortening of Y2–Ru decreases to only 0.090 Å for Y2–Os in the heavier analogue, while the average Y–Z distance increases only 0.011 Å ($\sim 3.5\sigma$). On the other hand, the cluster in $Y_6I_{10}Ir$ (Figure 1) is found to be elongated along Y3–Ir, although by only 0.035 Å. Any electronic effects associated with the nominal t_{1u}^5 HOMO in the iridium compound are not obvious in the distance spectrum. The observed distortion in the last is at least in a plausible direction in the absence of strong electronic effects, since condensation of the clusters into chains via pairs of parallel $I4^{i-i}$ and $Y3–I5^{a-i}$ interactions occurs in this direction.

A particular puzzle is the 56% decrease with osmium for what was once thought to be a plausible distortion in the isoelectronic ruthenium cluster. Clearly these effects are less well understood

(24) The anisotropic atom displacement parameters for all three $R_6I_{10}Z$ compounds exhibit some common and structure-related characteristics. The U_{11} value for I2 and the U_{33} parameter for I3 are always the largest in each structure, and these correspond to displacements normal to the planes of the $(Y1–I2^{a-i})_2$ and $(Y2–I3^{a-i})_2$ intercluster bridges, respectively. Likewise, U_{22} for I1 is the third largest U_{ii} value in all three cases, and this corresponds to a wagging of the only two-bonded I^i atom in the structure.

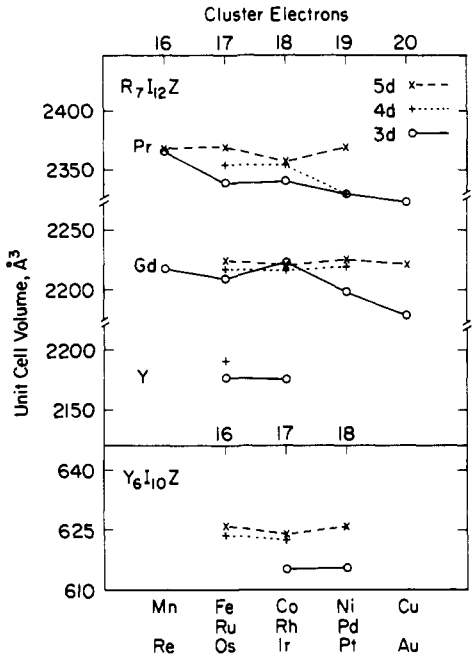

Figure 2. Unit cell volumes for all $R_7I_{12}Z$ and $Y_6I_{10}Z$ phases containing transition metal Z arranged by host R and the group of Z. The 3d, 4d, and 5d examples of Z are connected by solid, dotted, and dashed lines, respectively.

than we first conceived. A qualitative generalization regarding these unusual differences does come to mind, however. "Relativistic effects" are known to be markedly greater for the 5d elements,[25] and although a principal result is a tighter binding of the 6s orbitals, a secondary 5d orbital expansion is also recognized. The effect on 6s seems especially interesting, since the charge-consistent H_{ii} value for Ru 6s is high and off scale in the MO diagram published for $Y_6I_{10}Ru$.[26] What we may be seeing is a strengthening of the Y–Os bonds via more effective osmium 6s and 5d (nominally a_{1g} and t_{2g}) orbitals to the extent that these overshadow the Y–Y bonding that appears to dominate distortions from the ideal t_{1u}^4 HOMO in $Y_6I_{10}Ru$. The result would be a more nearly regular osmium cluster, as observed, with the distortion becoming negligible with one more electron in iridium.

$R_7I_{12}Z$ Cell Volumes. This structure originated with $Sc(Sc_6Cl_{12}N)$ and the like,[12] and iodide examples for R = Sc, Y, Pr, and Gd with Z = Mn–Ni have been described since.[10] The structure can be derived from cubic close-packed $R_6I_{12}Z$ clusters oriented with their $\bar{3}$ axes normal to the layers. The six edge-bridging iodines about the waist of each cluster are then exo-bonded to R vertices in clusters in the two adjacent layers, and vice versa. Finally, the seventh, isolated R^{III} atom lies on the $\bar{3}$ axis in all trigonal antiprismatic sites between pairs of clusters with the same stacking orientation so that the cation's neighbors are the other six edge-bridging iodines.

Although structural details are available for only $Sc_7I_{12}Co$ and $Y_6I_{12}Fe$ among the metal-centered examples, some ideas regarding distance and bonding variables can be secured by a consideration of unit cell volumes. Figure 2 shows these for all of $R_7I_{12}Z$ examples, R = Y, Pr, and Gd, as well as for the few $Y_6I_{10}Z$ examples. The presentation is organized by group (and therefore electron count) and is coded according to whether the interstitial is a 3d, 4d, or 5d member.

Several features of these volumes are unexpected. First, it is difficult to preceive in these data the expected increase in bonding within the clusters from the Mn to the Co families that would correspond to an increasing number of bonding electrons in the idealized t_{1u} HOMO. The same, contrary result applied for the expected decrease in bonding beyond this $18e^-$ optimum (above) for nickel and copper. The view that lattice size is determined largely by bond strength within the clusters is likely too simple, and a second thought might be that changes in the effective radii of Z in each period could be responsible. Interstitial volumes derived from metallic radii of Z[20] qualitatively reproduce the trends in each period quite well, including the upturn for Pt but not the decrease found with Cu and Au. On the other hand, these data do poorly in accounting for the rate of change within each family. Standard metallic (or crystal) radii as well as distances in the isostructural metals are quite similar for the 4d and 5d elements in each group, but these are appreciably greater (by ~0.1 Å or 8–10%) than those for each congenerous 3d member.

The close grouping of the $R_7I_{12}Z$ members of all three periods for each R (Figure 2) suggests that all volume variations, particulary within each family, do not simply and accurately reflect expected or presumed changes in cluster volumes. In fact, separations between clusters constructed from a given host element are known to be determined not solely by the size of the interstitials but by the lengths of the intercluster-bridging $M\text{--}X^{a-1}$ (or other types of) bonds at each metal vertex as well. The last have in turn been observed to exhibit distance properties that depend significantly on closed shell $X^a\cdots X^i$ repulsions or matrix effects[4,27] about each vertex rather than on $M\text{–}X^a$ bond properties alone. This is because metal–metal bonding draws these vertices inside the edge-centered cube defined by inner halogen or, alternatively, the halogen cube is expanded beyond the cluster vertices because of repulsions between these halogens. This distortion (matrix effect), which clearly increases with halogen size, can severely restrict the access of X^a to each R vertex, since X^a may first encounter the four edge-bridging X^i atoms that protrude about that point. Particularly with iodides this can mean that an increase in the size of Z (or R) does not result in a significant increase in the $R\text{--}I^a$ distance; rather, a more nearly normal bond distance to I^a is achieved while the cluster separations are relatively fixed by $I^a\cdots I^i$ contact distances. A striking effect of this character has been seen in the series of $R_7I_{12}Z$ phases involving the R–Z pairs Sc–Co, Y–Fe, and Pr–Co, where the $R\text{--}I^a$ distance increases just 0.04 Å while d(R–Z) is increasing 0.34 Å![10] Very much the same thing should happen in iodides when R is fixed and Z is varied. Thus, we conclude that the abnormally small changes in cell volumes between isoelectric 3d vs 4d and 5d examples (Figure 2) probably reflect a matrix effect, much of the cluster expansion that comes from the larger interstitials being soaked up by diminished $R\text{--}I^a$ distances. Horizontal trends in Figure 2 may be similarly obscured.

Although relatively simple matrix effects do account for the qualitative features observed for the cell volumes, many of the smaller trends seem inexplicable. A detailed examination would probably show that the R_6 trigonal antiprisms ("octahedra") also distort through changes in their height-to-basal-edge ratios. Such changes are suggested by the regular trend in the c/a ratios for the $R_7I_{12}Z$ cells, which usually decrease by 1–1.5% from the 3d to the later or heavier Z examples. It would be informative, but perhaps relatively tedious, to examine these structural effects in detail. The differences found within three $Y_6I_{10}Z$ examples characterized structurally are likewise not at all evident in their cell volumes (Figure 2).

Acknowledgment. Reactions that were later found to provide $Gd_7I_{12}Ni$, $Gd_7I_{12}Ru$, and $Y_6I_{10}Ni$ were first run by Tim Hughbanks. R. A. Jacobson is thanked for the continued provision of diffraction facilities. This research was supported by the National Science Foundation, Solid State Chemistry, via Grants DMR-8318616 and DMR-8902954 and was carried out in facilities of the Ames Laboratory, DOE.

Supplementary Material Available: Tables of data collection and refinement information and anisotropic thermal parameters for $Y_6I_{10}Os$ and $Y_6I_{10}Ir$ (3 pages); listings of observed and calculated structure factor data for these two compounds (39 pages). Ordering information is given on any current masthead page.

(25) Pyykkö, P.; Desclaux, J.-P. *Acc. Chem. Res.* **1979**, *12*, 276.
(26) The Ru 6s level is at −5.57 eV in Figure 4, ref 14.
(27) Corbett, J. D. *J. Solid State Chem.* **1981**, *37*, 335.